Xenoliths Evidence of Alkaline Magmatic Infiltrations Beneath Lake Nyos (Cameroon Volcanic Line, West Africa)

Merlin Isidore Teitchou, Joseph Legrand Tchop, Michel Grégoire, Pauline Wokwenmendam Nguet, Eddy Ferdinand Mbossi, Jacques Dili-Rake, Joseph Victor Hell

Scientific Research Publishing

Open Journal of Geology, 2022, 12, 433-459
https://www.scirp.org/journal/ojg
ISSN Online: 2161-7589
ISSN Print: 2161-7570

Xenoliths Evidence of Alkaline Magmatic Infiltrations Beneath Lake Nyos (Cameroon Volcanic Line, West Africa)

Merlin Isidore Teitchou[1*], Joseph Legrand Tchop[1], Michel Grégoire[2], Pauline Wokwenmendam Nguet[1], Eddy Ferdinand Mbossi[1], Jacques Dili-Rake[1], Joseph Victor Hell[1]

[1]Institute for Geological and Mining Research, Buea, Cameroon
[2]Geosciences-Environnement Toulouse, Toulouse, France
Email: *teitchou.merlin@yahoo.fr

How to cite this paper: Teitchou, M.I., Tchop, J.L., Grégoire, M., Nguet, P.W., Mbossi, E.F., Dili-Rake, J. and Hell, J.V. (2022) Xenoliths Evidence of Alkaline Magmatic Infiltrations Beneath Lake Nyos (Cameroon Volcanic Line, West Africa). *Open Journal of Geology*, **12**, 433-459.
https://doi.org/10.4236/ojg.2022.126021

Received: April 22, 2022
Accepted: June 13, 2022
Published: June 16, 2022

Abstract

Xenoliths enclosed in Lavas of the Nyos volcano (Cameroon Volcanic Line, continental sector) range from fertile lherzolites to harzburgites. One spinel-free wehrlite has been also sampled. The occurrence of phlogopites and pargasites in some harzburgites together with specific textural rock-type (lherzolites transitional porphyroclastic to equigranular), including major and trace element compositions both in peridotites bulk rocks and minerals point out interactions between the mantle and basaltic magmas responsible for the formation of wehrlites beneath the Nyos volcano. Hydrous minerals (phlogopites and pargasites) and metasomatic events are their main petrogeochemical signatures different from group 1 samples which are characterized by spoon-shaped REE patterns. Later on, hydrous phases, Ti-rich Cpx, CaO rich Ol, Ti, and V rich Ol wehrlite precipitated from melt enrichments due to the percolation of the mantle by basaltic magmas of alkaline affinity. The metasomatic liquid which percolates the Nyos mantle column was a dense alkaline silicate rich in volatile, displaying low HFSE abundances in the metasomatic hydrous melts compared to the LILE. It is suggested that Nyos mantle peridotites have experienced: 1) variable metasomatic events related to the percolating of the depleted mantle by a alkaline silicate liquid, 2) the spinel-free wehrlite is a group 2 sample corresponding to a cumulate of a similar melt, 3) amphibole may be a potassium-bearing mineral instead of or in addition to phlogopite at shallower levels of Nyos upper mantle and 4) transitional textural rock facies express also the fingerprint of rising mantle plume which were percolated by alkaline magma during their transit to the surface.

Keywords

Nyos, Wehrlites, Hydrous Minerals, Alkaline Silicate, Melt Percolation

1. Introduction

The Cameroon Volcanic Line (CVL; **Figure 1(a)**) is a chain of Tertiary to Recent, less tholeiitic, transitional to strongly alkaline intraplate volcanoes extending from the south Atlantic island of Pagalu to the continental interior of West Africa (Biu Plateau), trending averagely N30˚E and extending over a distance of 1600 Km [1] [2] [3]. The Nyos volcanic unit (6˚26'N and 10˚18'E) is part of the Oku massif, one of the continental CVL massifs. In this unit, volcanism has been concentrated in distinct eruptive centers, the largest one being to take in the Lake Nyos area. The Nyos volcanic rocks, mainly basalts have been grouped into two successive episodes. The first manifestation has been termed the first episode [4] and is made up of large basaltic lava flows. The second episode (recent series) activity contrasts with the relatively quiet volcanism of the earliest volcanic activity in that it was highly explosive, giving rise to steep pyroclastic cones and maars. A recent series is a group of craters, tuff cones, and flows which, on the basis of their youthful morphology, are regarded as the products of some of the most recent activity in Oku massif. The volcanism of the Lake Nyos area is essentially basic and different from that of the CVL continental swells which can be bimodal (basic and/or acid [4]. Lava flows, maar pyroclastics, and cinder cones from the Nyos volcano enclose abundant ultramafic xenoliths of spinel lherzolites and harzburgites and a diverse suite of crustal rock. Websterites have also been described by Temdjim *et al.* [5]. Ultramafic xenoliths have not been found in the first episode. Ultramafic xenoliths comprise varying combinations of olivine, orthopyroxene, clinopyroxene, spinel, and amphibole. New petrogeochemical investigations allow us to portrait special petrographic (wehrlites and lherzolites transitional porphyroclastic to equigranular) and mineralogic (pargasites and phlogopites) features and to precise their origin and highlight the alkaline affinity of the magma that brought out these peridotites.

2. Geological Setting and Xenolith Petrography

The geological setting of the Lake Nyos area (**Figure 1(b)**) has been revisited by Teitchou [4]. In addition, it is important to note that Lake Nyos constitutes the lower down part of the four massifs (Babanki, Oku, Nkambe, and Nyos) which form mounts Oku (CVL). Volcanic formations of Lake Nyos, principally lava flows and maar deposits, rest uncomfortably over Pan-African metamorphic formations (mostly biotite gneiss) intruded by granitoids. Petrochemical data [6] [7] [8] point out that lavas of the Nyos volcano area are essentially basaltic and tholeitic and outlet by a low degree of partial melting as most lavas of the continental volcanic plains of the CVL formed in lower asthenospheric mantle

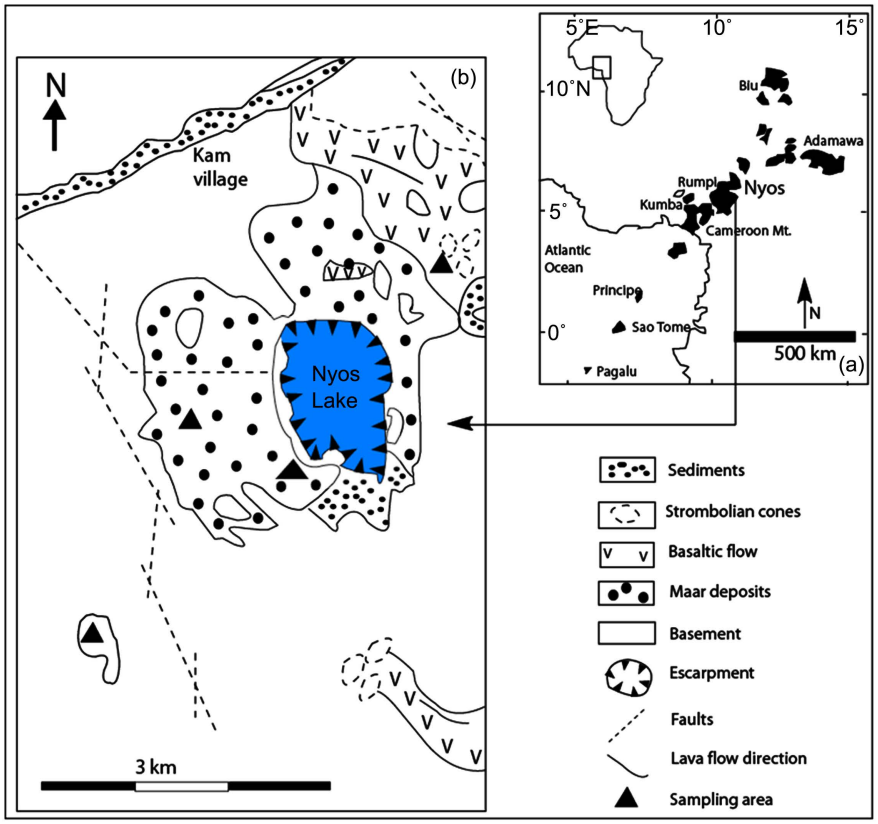

Figure 1. (a) Localization of the Cameroon volcanic line and (b) geological map of the Lake Nyos volcanic unit area.

sources [9]. Lavas are sodic and share some OIB characteristics. Basaltic lavas of the lake Nyos volcanic unit display petrological and geochemical similarities with other continental plains of the CVL, especially those of Kumba, Tombel and Noun [4].

Peridotite xenoliths recovered from Nyos area are found in recent lava flows and maar pyroclastics. These xenoliths can be enclosed in stratified deposits or in base surges ejecta, sometimes, occupying the heart of basaltic bombs. They also form real bombs of variety lengths up to 10 cm. The contact with the host lavas generally is sharp. Unbreaking bombs can be spherical, angular or ovoid.

Modal compositions of peridotites (**Table 1**) were determined following the method described by Teitchou *et al.* [10] [11]. Modal compositions, using Streckeisen diagram [12] allow recognizing lherzolites, harburgites and a free wehrlite (**Figure 2**).

Spinel lherzolites (samples NK01, NK05, NK07, NK09, NK11, NK13 and NK14) are the most abundant xenoliths in Nyos volcanic unit (more than 60% of collected samples) and are composed of olivine (55% - 70%), orthopyroxene (7% - 30%), clinopyroxene (6% - 20%) and spinel (1% - 6%). Harzburgites (samples NK02, NK04, NK10a, NK10b and NK15) are less abundant (30%) and are composed of olivine (71% - 83%), orthopyroxene (10% - 20%) and clinopyroxene (2% - 4%). Studied lherzolites and harzburgites have predominantely

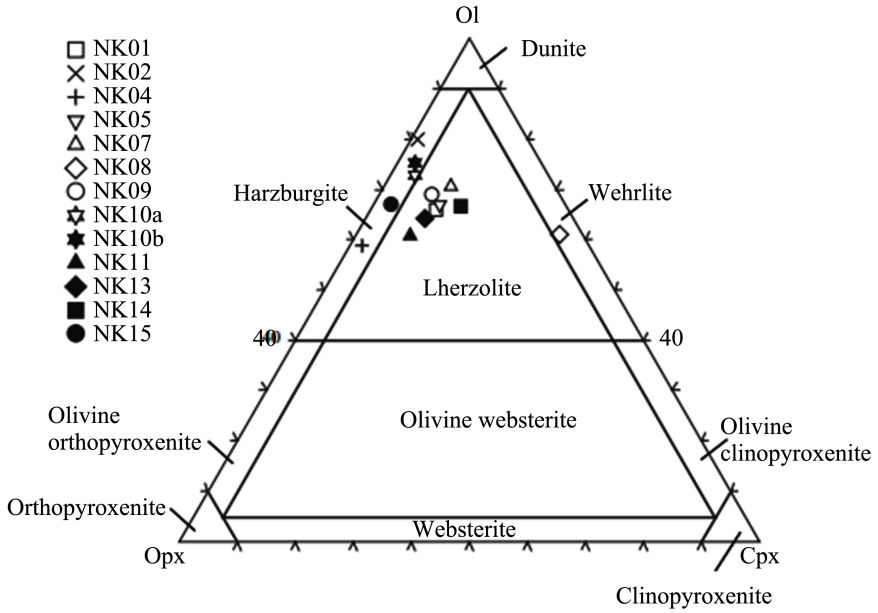

Figure 2. Modal composition of the studied Nyos xenoliths. Classification is after [12]. Ol—olivine; Opx—orthopyroxene; Cpx—clinopyroxene.

Table 1. Modal compositions of the investigated Nyos mantle peridotites (in vol%).

Sample	Olivine	Orthopyroxene	Clinopyroxene	Spinel	Amphibole	Phlogopite
NK01	67	22	8	3	-	-
NK02	80	19	1	trace	1	-
NK04	73	20	2	3	-	2
NK05	71	16	9	4	-	-
NK07	67	17	11	5	-	-
NK08	63	-	37	-	-	-
NK09	60	19	8	3	-	-
NK10a	70	22	4	4	-	-
NK10b	73	21	3	3	-	-
NK11	69	22	8	1	-	-
NK13	63	25	10	2	-	-
NK14	66	18	15	trace	-	-
NK15	65	29	3	2	-	-

porphyroclastic and protogranular textures respectively, except wehrlite NK08 (modal composition: Ol: 63, Cpx: 36 and glass patches or veinlets < 1%) which is the only sample that displays a cumulative texture mostly consisting of sub-euhedral olivines associated to interstitial anhedral clinopyroxenes commonly poekilitic. Wehrlite also contains localy a strip of clinopyroxene which cristallyse in disavantage of orthopyroxene (**Figure 3**). Similar processes transforming

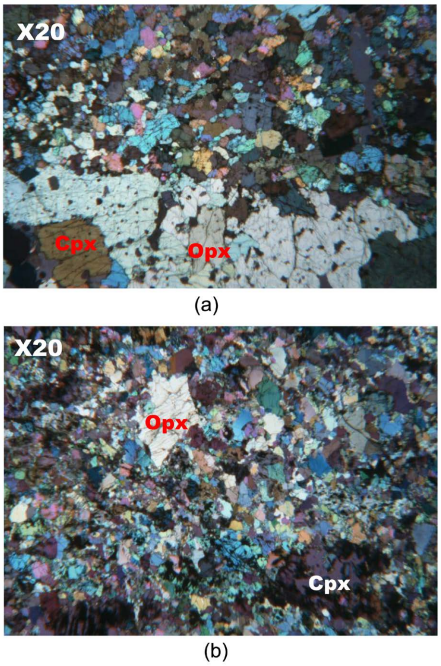

Figure 3. Microphotographs of (a) wehrlite NK08 show a strip of Cpx which crystallize in favor of Opx; (b) lherzolite NK14 showing transitional porphyroclastic to equigranular texture.

Opx into Cpx have been reported in other peridotite xenolith occurrences in the world, e.g. by Boivin [13] in composite xenoliths of Tallante in Spain), Neuman and Wulf-Pederson [14], lherzolites of Canaries Islands, Grégoire *et al.* [15] in harzburgites of Kerguelen Islands and Remaïdi [16] in lherzolitic massif of Ronda. Sample NK14 have transitional porphyroclastic to equigranular texture and displays pyroxene-Cr spinel symplectites with CO_2 inclusions.

3. Analytical Methods

Major and trace elements of minerals were analysed at the UMR 5563 (LMTG, Observatoire Midi-Pyrénées) of University Paul Sabatier (Toulouse III, France). Major-element compositions of minerals were determined with the CAMECA SX50 electron microprobe and a standard program: beam current of 20 nA and acceleration voltage of 15 kV, 10 to 30 s/peak, 5 - 10 s/background counting times, and natural and synthetic minerals as standards. Nominal concentrations were subsequently corrected using the PAP data reduction method [17]. The theoretical lower detection limits are about 100 ppm (0.01%). The concentrations of Rare Earth Elements and other trace elements (La, Ce, Pr, Nd, Sm, Eu, Gd, Tb, Dy, Ho, Er, Yb, Lu, Rb, Ba, Th, Sr, Zr, Ti, Y, Ni, V and Sc) in clinopyroxenes and amphiboles were analysed in situ on 100 - 120 mm thick polished sections with a Perkin-Elmer Elan 6000 ICP-MS instrument coupled to a CETAC laser ablation module that uses a 266 nm frequency-quadrupled Nd-YAG laser. The NIST 610 and 612 glass standards were used to calibrate relative ele-

ment sensitivities for the analyses. The analyses were normalized using CaO values determined by electron microprobe. The analyses were performed on inter-cleavage area from the cores of the freshest cpx and amphibole grains in order to get homogeneous results unaffected by alteration or exsolution processes. A beam diameter of 50 - 100 μm and a scanning rate of 20 μm/s were used. The typical relative precision and accuracy for a laser analysis range from 1% to 10%. Typical theoretical detection limits range from 10 to 20 ppb for REE, Ba, Rb, Th, Sr, Zr and Y; 100 ppb for Sc and V; and 2 ppm for Ti and Ni (see in Dantas *et al.* [18] for more details).

Major element compositions of the same sample were carried out with XRF techniques (Philips 2400) and measured on fused disks at Saint-Etienne school of Mines, France.

Trace element composition in Nyos peridotites were obtained using ground rock powders (~100 mg) dissolved in HF-HNO_3 mixtures. Dried samples were taken up in HNO_3 and diluted to 1:1000 in 2% HNO_3. Reference sample BEN was used for calibration. Chemical blanks and 2 reference materials (UB-N, JP-1) were run with each sample batch.

4. Mineral Chemistry

Nyos peridotites display four typical mantle minerals: olivine, orthopyroxene, clinopyroxene and spinel. Disseminated dark pargasitic amphibole and brown phlogopite plates are observed in harzburgites NK02 and NK04 respectively.

4.1. Major Element Distribution

Selected electron microprobe analysis of minerals phases are given in **Tables 2(a)-(e)**.

Olivine compositions in lherzolites and harzburgites range between Fo_{87} and Fo_{91} (mole %) and CaO contents are 0.07% - 0.09% (wt%). Magnesium rich olivine appears in harzburgites with $Fo_{88\text{-}91}$. Harzburgites have high NiO contents (0.30 - 0.45 wt%) like ophiolitic and oceanic ridge peridotites [19] [20]. High NiO and Fo contents of harzburgites are mineralogical fingerprints of their refractory characters [21]. Wehrlite NK08 has low Fo contents ($Fo_{79.17\text{-}78.75}$) and is rich in CaO (mean composition: 0.45 wt%) in comparison to lherzolites and harzburgites. Wehrlite NK08 and lherzolite transitional porphyroclastic to equigranular NK14 have low NiO content compare to harzburgites and porphyroclastic lherzolites.

Orthopyroxenes plot in the field of enstatite ($En_{89.97\text{-}86.63}$) with narrow variation of Mg# (=100 × Mg/Mg + Fe_{total}, between 88.26 - 90.88). Orthopyroxene of Nyos peridotites are similar to those described by Caldeira and Munha [22] in São Tomé islands and by Tamen [23] in Mandara massifs, respectively in the oceanic and continental sectors of the CVL.

Diopsidic clinopyroxenes of Nyos ($En_{48.44\text{-}41.02}$ - $Fs_{11.50\text{-}4.83}$ - $Wo_{47.48\text{-}46.16}$) are rich in Cr_2O_3 (until ~1.3%) and Al_2O_3: 3.22% à 8.10%. Mg# Cpx increase from wehrlite

Table 2. (a) Representative microprobe analyses of cores of olivines; (b) Representative microprobe analyses of cores of orthopyroxenes; (c) Representative microprobe analyses of cores of clinopyroxene; (d) Representative microprobe analyses of cores of spinel; (e) Representative microprobe analyses of cores of amphibole.

(a)

	Group 1 Lherzolite	Group 1 Lherzolite	Group 1 Lherzolite	Group 1 Lherzolite	Group 1 Harzburgite	Group 1 Lherzolite	Group 1 Harzburgite	Group 1 harzburgite	Group 2 harzburgite	Group 2 Lherzolite	Group 2 Wehrlite
Olivine	NK01	NK05	NK07	NK09	NK10	NK11	NK15	NK02	NK04	NK14	NK08
SiO_2 (wt%)	40.90	41.10	41.71	40.82	41.03	41.44	41.64	41.29	40.51	40.87	38.95
TiO_2	0.03	-	-	-	0.01	-	-	-	0.03	-	0.01
Al_2O_3	-	-	-	-	-	-	-	-	-	-	-
Cr_2O_3	0.04	0.01	0.01	0.03	0.01	0.02		0.02		0.02	0.03
FeO_{total}	10.10	9.90	9.95	9.66	9.66	9.84	9.95	9.58	12.20	12.57	19.86
MnO	0.13	0.15	0.13	0.1	0.13	0.12	0.19	0.15	0.16	0.19	0.30
MgO	49.59	50.08	49.49	49.87	49.94	49.19	49.48	49.81	47.62	47.38	41.81
CaO	0.09	0.09	0.12	0.06	0.11	0.11	0.06	0.09	0.07	0.09	0.26
NiO	0.36	0.37	0.39	0.32	0.29	0.25	0.38	0.32	0.45	0.17	0.04
Total	101.23	101.66	101.79	100.85	101.17	100.98	101.71	101.26	101.04	101.29	101.25
Mg#	89.75	90.02	89.86	90.20	90.21	89.91	89.86	90.26	87.43	87.04	78.95

(b)

Orthopyroxene	NK01	NK05	NK07	NK09	NK10	NK11	NK15	NK02	NK04	NK14
SiO_2 (wt%)	55.43	55.36	57.10	56.48	55.70	56.06	56.62	56.76	55.93	54.56
TiO_2	0.06	0.04	0.01	0.05	0.04	-	0.06	0.01	0.04	0.13
Al_2O_3	4.34	4.46	3.74	3.65	3.75	3.66	3.79	3.23	2.43	-
Cr_2O_3	0.40	0.46	0.29	0.33	0.39	0.35	0.40	0.46	0.40	0.47
FeO_{total}	6.53	6.44	6.59	6.58	6.22	6.51	6.39	5.99	7.81	7.83
MnO	0.13	0.13	0.12	0.13	0.17	0.10	0.16	0.11	0.12	0.21
MgO	33.44	33.34	33.76	33.61	34.02	33.33	33.63	33.8	32.95	32.44
CaO	0.76	1.32	0.76	0.60	0.57	0.74	0.63	0.77	0.85	0.81
Na_2O	-	0.01	-	-	-	-	-	-	-	-
K_2O	-	0.01	-	0.01	0.01	-	-	-	-	-
Total	101.19	101.74	102.37	101.45	100.98	100.76	101.66	101.13	100.63	100.51
Mg#	90.13	90.21	90.13	90.11	90.70	90.12	90.36	90.96	88.27	88.08

(c)

Clinopyroxene	NK01	NK05	NK07	NK09	NK10	NK11	NK15	NK02	NK04	NK14	NK08
SiO_2 (wt%)	52.19	52.43	52.47	52.26	51.74	52.45	53.45	52.46	52.90	52.13	47.68
TiO_2	0.25	0.20	0.30	0.27	0.41	0.32	0.31	0.25	0.22	0.50	1.77
Al_2O_3	5.34	5.37	5.67	5.13	5.98	5.70	5.13	4.40	3.22	4.54	8.10
Cr_2O_3	0.72	0.66	0.79	0.63	0.85	0.81	0.78	1.26	0.71	1.10	0.14
FeO_{total}	3.07	3.10	3.17	2.96	2.84	3.08	2.78	3.07	3.36	4.05	6.67
MnO	0.10	0.07	0.10	0.093	0.08	0.043	0.09	0.10	0.07	0.13	0.16
MgO	16.11	16.28	15.75	16.05	15.12	15.68	15.84	16.19	16.61	15.90	13.35
CaO	22.05	21.69	21.65	21.94	21.56	21.53	21.67	21.70	23.15	21.69	21.50
Na_2O	0.88	1.09	1.02	1.07	-	1.11	1.24	0.81	0.43	0.90	0.63
K_2O	-	0.01	-	-	-	0.01	0.01	0.02	0.04	0.01	-
Total	100.72	100.89	100.92	100.62	98.58	100.73	101.31	100.24	100.72	100.94	99.98
Mg#	90.33	90.35	89.86	92.97	90.47	90.07	91.03	90.38	89.79	87.50	78.10

(d)

Spinel	NK01	NK05	NK07	NK09	NK10	NK11	NK15	NK02	NK04	NK14
SiO_2 (wt%)	0.05	0.03	0.04	0.03	0.02	0.04	0.03	0.05	0.06	0.07
TiO_2	0.03	0.03	0.06	0.03	0.03	0.04	0.06	0.04	0.36	0.53
Al_2O_3	55.08	55.67	54.91	55.48	55.32	55.21	54.82	38.46	35.63	31.79
Cr_2O_3	11.64	11.3	11.49	11.47	11.94	11.32	12.43	27.99	27.15	29.85
Fe_2O_3	3.78	3.98	3.99	3.08	3.01	3.42	2.25	6.49	6.54	8.94
FeO	9.76	9.20	9.32	9.47	9.39	9.36	9.37	9.38	15.11	14.11
MnO	0.12	0.11	0.11	0.10	0.07	0.11	0.11	0.16	0.16	0.18
MgO	20.13	20.63	20.40	20.28	20.39	20.26	20.09	17.52	14.54	15.20
ZnO	0.08	-	-	-	-	-	0.06	-	0.24	-
NiO	0.36	0.43	0.34	0.33	0.28	0.41	0.37	0.18	0.27	0.26
Total	101.03	101.39	100.67	100.26	100.44	100.16	99.57	100.26	100.06	100.91
Mg#	73.16	74.20	73.80	74.70	75.07	74.38	75.86	67.23	55.25	55.01
Cr#	12.42	11.99	12.31	12.18	12.65	12.09	13.21	32.81	33.82	38.65

(e)

Amphibole	NK02	Phlogopite	NK04
SiO_2 (wt%)	43.74	SiO_2 (wt%)	38.62
TiO_2	1.40	TiO_2	2.92
Al_2O_3	13.56	Al_2O_3	15.84
Cr_2O_3	2.10	Cr_2O_3	0.92

Continued

FeOtotal	4.07	FeO_{total}	4.59
		ZnO	0.03
MnO	0.07	MnO	0.05
MgO	17.43	MgO	22.20
CaO	11.07	CaO	0.01
Na_2O	3.09	Na_2O	0.54
K_2O	1.15	K_2O	9.45
		BaO	0.29
NiO	0.08	NiO	0.23
Total	97.75	Total	95.69
Mg#	88.42	Mg#	89.61

(Mg#: 78.10) to lherzolites and harzurgites (Mg#: 87.50 - 90.86). Al_2O_3 content of Cpx is high in wehrlite (Al_2O_3: 8.10%) compare to lherzolites and harzburgites (3.22% - 5.71%) and therefore express a disequilibrium in the initial gathering or paragenesis of minerals. Cpx of Nyos xenoliths have low Ti contents (~0.01) except wehrlite NK08 (Ti = 0.05). Cr contents increase from wehrlite (0.01) to harzburgites (0.04). Cpx of Nyos peridotites are similar to those of Lake Nji peridotites in the volcanic area of Mount Oku [24] which belong to the continental sector of CVL.

Spinels Mg# (=100 × Mg/Mg + Fe^{2+}) and Cr# (=100 × Cr/Cr + Al) are in the range 55 - 78 and 12 - 39 respectively. Al_2O_3 (31.79% - 55.48%) and Cr_2O_3 (11.20% - 29.85%) contents vary widely. TiO_2 contents are very low (<0.4%) except for lherzolite NK14 with mean composition is 0.53%. Porphyroclastic lherzolites display a fertile character (Cr# < 13) while lherzolite NK14 and harzburgites display refractory character (Cr# > 31). Consequently, Porphyroclastic lherzolites contain Al spinel interpreted as residues of relative low degree of partial melting of the mantle component [25] while harzburgites and lherzolite NK14 defines Cr spinel, witnesses of an important degree of partial melting compare to Al spinel. Low values of Cr# and medium to high values of Mg# excluded a magmatic origin of these minerals. Thus, most peridotites of Nyos seem to have experienced a low degree of partial melting, attested by the low proportion of harburgites and the absence of dunites. Spinels of Nyos volcanic unit are similar to those of the Loihi Seamount [26] and comparable to those of Adamawa mantle xenoliths [27].

Sample NK02 contain calcic amphibole (Ca/Na > 1; Ca + Na > 1.34 and Na < 0.67; Al^{IV} > Fe^{3+}) and therefore correspond to pargasite [28]. Nyos pargasitic amphibole have slightly high MgO (15.08% - 17.77%), TiO_2 (1.12% - 1.62%), Na_2O (2.97% - 3.17%), Cr_2O_3 (2.03% - 2.21%) and low K_2O (1.06% - 1.26%) contents. Al_2O_3 (13.43% - 13.66%) and Mg# (98) contents are less variable. Nyos

pargasites are similar to those of equigranular lherzolites of Orania [29] and different of brown metasomatised amphibole of the Caussou in French Pyrénées [30].

Phlogopites occur as sub-euhedral grains along grain boundaries in lherzolite xenoliths or along orthopyroxene lamellae exsolved from intercumulus clinopyroxene in the wehrlite xenoliths. They do not show any reaction relationships with other phases in any of the xenoliths studied indicating that the phlogopites have equilibrated with these coexisting phases. Phlogopites (Fe/Fe + Mg: 0.10 to 0.11) in sample NK04 have high TiO_2 (~3%) and low Cr_2O_3 (<1%) contents. They have Mg/Mg + Fe^{2+} similar to that of coexisting olivine, clinopyroxene, and orthopyroxene and are similar to phlogopites of type I wehrlite of Oranie describe by Zerka *et al.* [31].

4.2. Trace Element Distribution

LA-ICP-MS analyses of mineral phases are given in **Table 3(a)** and **Table 3(b)**. In general, olivines, orthopyroxenes and spinels have REE contents below the detection limit except for transitional elements whereas clinopyroxenes and amphiboles are rich in trace elements and micas remain poor in REE.

4.2.1. Olivines

Transition element concentrations are homogeneous or less variable (Sc: 4.5 - 6 ppm; Ti: 42 - 49 ppm; Ni: 2740 - 3090 ppm). Olivine wehrlite is slightly rich in Ti (125 ppm) but poor in Ni (830 ppm). Its vanadium content (17 ppm) is higher compare to olivine bearing lherzolites and harzburgites which are below the detection limit. Incompatible trace elements have generally low concentrations or stand below the detection limit. Wehrlite NK08 and lherzolite NK14 are slightly rich in REE than other peridotites.

4.2.2. Orthopyroxenes

Sc (19 - 23 ppm) and V (105 - 125 ppm) contents of orthopyroxenes are closer to Cl chondrites while their Ni (709 - 759 ppm) content are higher. They also display a low composition of Sr (0.3 - 0.5 ppm), Zr (0.3 - 0.7 ppm), Ti (435 - 590 ppm) and Y (0.8 - 1.2 ppm). HREE contents are generally less variable ($[Yb]_N$: 0.5 - 0.9).

4.2.3. Clinopyroxenes

Transitional element concentration of clinopyroxene (Sc: 55 - 74 ppm; V: 135 - 255 ppm; Ni: 228 - 276 ppm) are relatively less variable in lherzolites and harzburgites while wehrlite clinopyroxenes have high V (295 ppm), low Ni (102 ppm) and equivalent Sc (70 ppm) contents. Ti contents yield broad variation ranges, varying from 460 ppm in harzburgite bearing phlogopite NK02 to 10465 ppm in wehrlite NK08.

Clinopyroxenes from selected Nyos xenoliths, normalised to the estimated primitive mantle values [32] display three distinct REE patterns (**Figure 4(a)**): 1) "spoon" shape patterns or group 1 samples characterized by HREE enriched

Table 3. (a) Representative clinopyroxene trace-element analyses (LA-ICP-MS) of Nyos peridotites (values in ppm); (b) Representative amphibole and phlogopite trace-element analyses of Nyos peridotites (values in ppm).

(a)

	Group 1 Harzburgite	Group 1 Harzburgite	Group 1 Harzburgite	Group 1 Lherzolite	Group 1 Lherzolite	Group 1 Lherzolite	Group 1 Lherzolite	Group 2 Lherzolite	Group 2 Larzburgite	Group 2 Wehrlite
Sample	NK02	NK10	NK15	NK01	NK05	NK09	NK11	NK14	NK04	NK08
Sc	66.35	61.48	73.91	61.72	60.97	57.78	58.04	55.11	55.56	69.58
Ti	461.98	1608.62	2006.4	1702.56	1643.34	1799.66	1847.82	3563.77	1182.25	10,465.00
V	151.82	229.97	254.97	230.11	218.95	226.07	228.39	248.55	134.55	295.46
Ni	228.38	289.01	256.10	276.37	249.36	272.56	271.42	247.02	247.58	101.95
Rb	0.77	2.94	0.77	2.88	3.27	2.39	3.75	3.16	1.18	1.39
Sr	147.23	18.53	6.23	20.03	20.18	12.17	11.86	125.28	102.61	98.73
Y	13.40	15.40	16.08	16.21	16.31	14.72	18.32	15.11	10.11	10.29
Zr	19.32	12.12	7.41	12.17	12.92	9.32	13.56	56.22	108.46	78.05
Nb	0.37	0.21	0.08	0.25	0.20	0.13	0.21	0.59	0.17	0.94
Ba	7.37	26.40	2.82	26.53	33.26	20.66	34.77	29.32	9.13	5.79
La	13.26	1.67	0.09	1.70	1.44	0.26	0.51	9.43	8.04	6.15
Ce	22.05	2.37	0.29	2.47	1.83	0.68	0.96	23.18	30.15	17.46
Pr	2.01	0.25	0.09	0.24	0.20	0.16	0.12	3.28	5.53	2.93
Nd	6.90	1.48	1.07	1.31	1.04	1.37	1.18	15.12	28.22	15.80
Sm	1.51	0.82	0.71	0.72	0.66	0.81	0.78	4.34	6.94	4.99
Eu	0.51	0.40	0.41	0.38	0.35	0.40	0.43	1.42	1.71	1.68
Gd	1.71	1.55	1.69	1.63	1.51	1.55	1.85	3.81	4.27	4.75
Dy	2.13	2.20	2.42	2.29	2.25	2.13	2.50	3.51	3.77	4.28
Ho	0.47	0.52	0.58	0.55	0.55	0.50	0.58	0.70	0.62	0.75
Er	1.35	1.59	1.65	1.65	1.64	1.49	1.66	1.78	1.46	1.63
Yb	1.40	1.58	1.58	1.58	1.57	1.50	1.59	1.59	1.21	1.28
Lu	0.20	0.22	0.22	0.22	0.21	0.21	0.23	0.22	0.15	0.14
Hf	0.45	0.50	0.47	0.51	0.54	0.49	0.65	1.31	2.93	3.59
Ta	0.01	0.02		0.03	0.03	0.01	0.02	0.07	0.03	0.14
Th	0.34	0.26	0.03	0.34	0.37	0.08	0.22	0.81	0.38	0.21
U	0.23	0.16	0.03	0.16	0.22	0.10	0.17	0.27	0.07	0.08

(b)

	Group 1 Amphibole Amp harzburgite NK02	Group 2 Phlogopite Phl harzburgite NK04
Sc	43.78	8.79
Ti	2132.40	17,412.84

Continued

V	207.7	212.70
Ni	295.63	1333.66
Rb	3.03	360.97
Sr	136.21	137.34
Y	13.50	0.23
Zr	32.43	17.94
Nb	9.06	8.75
Ba	31.24	2973.66
La	12.08	-
Ce	20.30	0.32
Pr	2.09	-
Nd	7.18	0.21
Sm	1.49	0.45
Eu	0.52	0.12
Gd	1.71	0.10
Dy	2.06	-
Ho	0.45	-
Er	1.35	0.03
Yb	1.40	0.05
Lu	0.21	-
Hf	0.81	0.54
Ta	0.41	0.58
Th	0.45	0.05
U	0.16	0.05

compare to MREE and LREE; $[La/Sm]_N$: 0.08 - 1.48; $[Sm/Yb]_N$: 0.47 - 0.57 and $[La/Yb]_N$: 0.03 - 0.69. Corresponding rocks are porphyroclastic lherzolites and harzburgites NK10. 2) "convex" shape patterns enriched in LREE and MREE compare to HREEs; $[La/Sm]_N$: 0.72 - 1.36; $[Sm/Yb]_N$: 2.85 - 6.23 et $[La/Yb]_N$: 3.27 - 4.52. Corresponding peridotites are lherzolite transitional to porphyroclastic NK14, wehrlite NK08 and phlogopite bearing harzburgites, sample NK04. 3) convex shape patterns enriched in LREE and display flat MREE and HREE patterns, corresponding rock is harzburgite bearing amphibole NK02 ($[La/Sm]_N$: 5.50; $Sm/Yb]_N$: 1.17 and $[La/Yb]_N$: 6.45).

Globaly, clinopyroxenes trace element patterns of Nyos can be divided in two groups, those enriched in LREE (type ii and iii) and those depleted in LREE (type i).

Nearly, all Nyos clinopyroxenes have deep negative anomalies of Ti and Nb and positive anomalies in U and Th (**Figure 4(b)**).

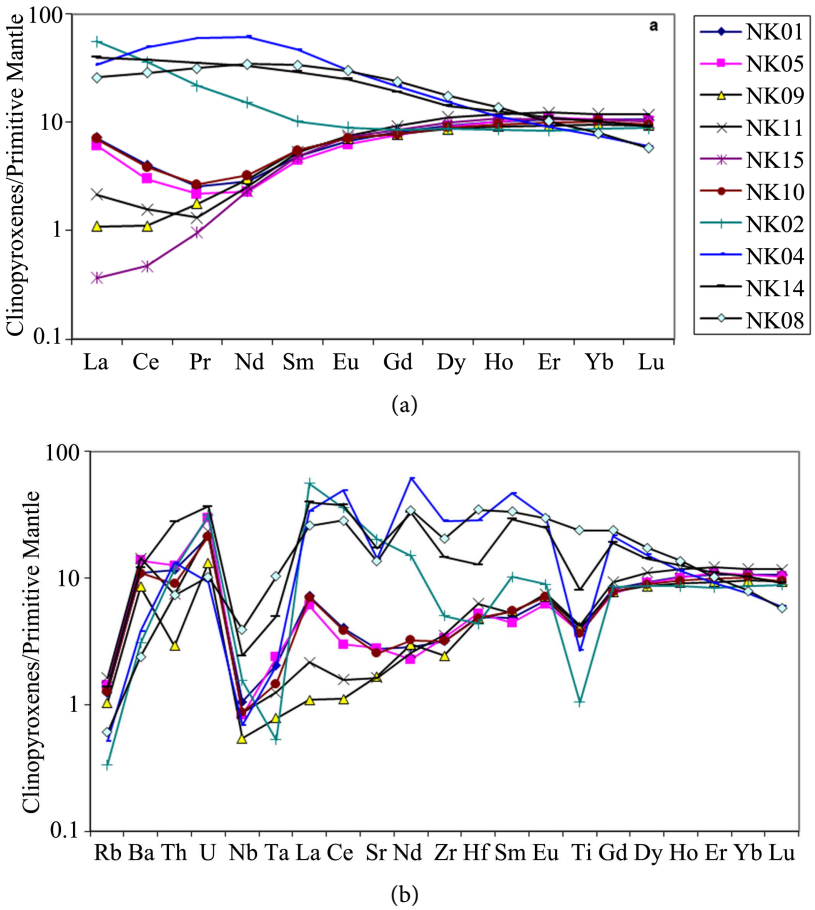

Figure 4. Clinopyroxene REE (a) and multi-element abundance (b) patterns normalised to the estimated primitive mantle values of Nyos peridotites. Normalization values after [32].

4.2.4. Amphiboles and Phlogopites

Transitional element contents in pargasitic amphibole are medium (Sc: 44 ppm; V: 208 ppm; Ni: 296 ppm) while Ti (2132.40 ppm) content is high like other incompatible elements. Analysed amphiboles point out REE enriches compare to the estimated primitive mantle values after McDonough and Sun [32]. They display enriched LREE compare to MREE and HREE; $[La/Sm]_N$: 5.08; $[Sm/Yb]_N$: 1.16 and $[La/Yb]_N$: 5.89. Nyos amphiboles are similar to those of Orania in Algeria [29].

In general, phlogopites have high contents of Ti (17,413 ppm), Ni (1334 ppm), V (213 ppm), Ba (2974 ppm) and Rb (361 ppm) while their Pr, Dy, Ho and Lu contents are below the detection limits. Phlogopites remain poor in REE (less than 1% of the estimated primitive Cl chondrites).

5. Bulk-Rock Geochemistry

5.1. Major Element Distribution

Analysed xenoliths by XRF technics and ICP-MS solution have generally homogeneous compositions (Table 4). Their Mg# = (100 × Mg/Mg + Fe_{total}) vary from

Table 4. Bulk Rock major-element data (X-Ray fluorescence) and trace-element data (ICP-MS solution) of Nyos peridotites.

	Group 1 Lherzolite	Group 1 Lherzolite	Group 1 Lherzolite	Group 1 Harzburgite	Group 2 Phl-Harzburgite
	NK01	NK05	NK11	NK10	NK04
SiO_2	43.59	43.74	45.4	44.1	45.94
TiO_2	0.07	0.07	0.08	0.08	0.11
Al_2O_3	2.7	2.77	3.09	2.89	1.68
Fe_2O_3	8.93	8.5	8.38	9.12	10.32
MnO	0.14	0.14	0.14	0.15	0.16
MgO	40.91	41.29	40.31	41.16	40.18
CaO	2.63	2.64	2.39	2.72	0.94
Na_2O	-	-	-	-	-
K_2O	-	-	-	-	0.03
P_2O_5	0.02	0.02	0.01	0.02	0.03
Total	99	99.17	99.79	100.23	99.39
Mg#	89.09	89.64	89.56	88.95	87.41
Sc	14.35	15.02	17.00	18.84	11.30
Ti	431.64	413.66	485.60	455.62	641.47
V	64.80	66.60	68.80	70.70	37.90
Cr	2844.20	2652.80	2910.00	2972.50	2934.20
Co	110.30	110.20	102.40	109.70	123.00
Ni	2145.60	2238.90	2040.70	2181.70	1983.20
Cu	15.60	5.9	2.70	16.60	24.20
Zn	53.20	46.00	48.90	63.30	64.50
Ga	1.32	1.61	1.80	1.88	1.92
Rb	0.06	0.04	0.032	0.07	3.29
Sr	2.98	1.32	0.50	3.14	4.34
Zr	1.18	0.64	0.84	1.28	6.55
Nb	0.15				0.19
Ba	2.96	1.09	1.37	3.76	31.37
La	0.45	0.23	0.20	0.60	0.59
Ce	0.59	0.32	0.31	0.87	1.50
Pr	0.07	0.04	0.04	0.11	0.24
Nd	0.35	0.24	0.22	0.49	1.13
Sm	0.11	0.10	0.09	0.16	0.28

Continued

Eu	0.05	0.05	0.04	0.07	0.08
Gd	0.23	0.21	0.23	0.26	0.20
Tb	0.04	0.04	0.05	0.05	0.03
Dy	0.32	0.31	0.37	0.40	0.19
Ho	0.08	0.08	0.09	0.09	0.04
Er	0.24	0.23	0.28	0.31	0.11
Tm	0.04	0.03	0.04	0.04	0.02
Yb	0.25	0.25	0.30	0.32	0.12
Lu	0.04	0.04	0.05	0.05	0.02
Th	0.04	0.04		0.04	0.04
U	0.01	0.02	0.01	0.02	0.02

86.20 to 88.53. Harzburgites NK04 and NK10 with Mg# < 88, respectively 86.20 and 87.87, are classified as ferric mantle peridotites while lherzolites with Mg# > 88 are considered as normal mantle peridotites [33].

K_2O and P_2O_5 contents are closed to the detection limit while Na_2O contents are null. K_2O contents are also null except for harzburgite bearing phlopopite NK04 (K_2O: 0.03) also characterized by low Al_2O_3 (<2%), CaO (<1%) and TiO_2 (<0.2%) contents which reflect lacking in Cpx and Sp.

Harzburgites have Al_2O_3/CaO ratio inferior to 1.1; estimated value for fertile mantle by Jagoutz *et al.* [34] or 1.2 proposed by McDonough and Frey [35]. These particularities are indication of their depleted or refractory characters. Nyos harzburgites are similar to harzburgitic xenoliths of Kerguelen [15] and Canaries islands [36].

Lherzolites show a relative homogeineity of their Mg# (88.02 - 88.62) and Al_2O_3/CaO (1.0 - 1.3) ratios and display a composition similar to the estimated fertile mantle. They have Cr# Sp < 13 and high Al_2O_3 and CaO contents. Nyos lherzolites are similar to that of the Barombi Mbo in the Kumba plain [10].

5.2. Trace Element Distribution

Analysed lherzolites and harzburgites are depleted in REE compare to the estimated primitive mantle values [32] except harzburgite NK04 which concentrations vary up to 5% of chondrites. The 2 harzburgites analysed are enriched in LREE compare to lherzolites. In general, 2 types of REE patterns (**Figure 5**) are identified:

1) Lherzolites and harzburgites NK10 have "spoon shape" REE patterns (**Figure 5(a)**) and display LREE depletion compare to MREE and less depleted HREE; ($[La/Sm]_N$: 1.37 - 2.53; $[Sm/Yb]_N$: 0.33 - 0.47 et $[La/Yb]_N$: 0.46 - 1.28). A slight La-Ce "inflexions" is observed. Their multi-element REE patterns (**Figure 5(b)**) are similar and characterize by positive anomalies in Nb, Ti and Sr and negative anomalies in U, La and Nd.

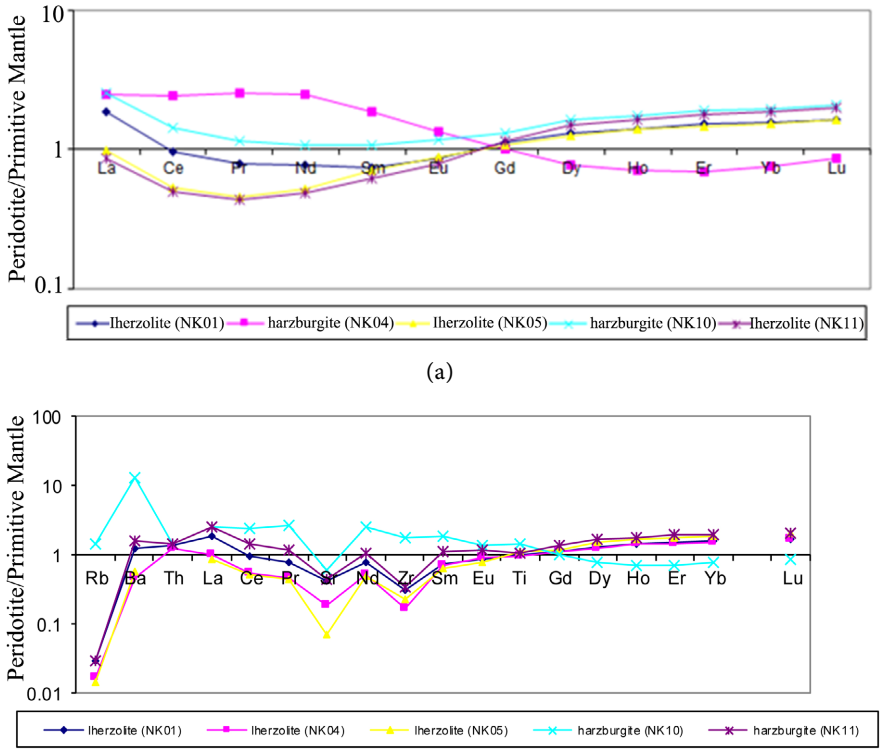

Figure 5. Bulk rock REE (a) and multi-element (b) patterns of Nyos péridotites.

2) Phlogopite REE patterns of harzburgite NK04 are characterised by a "convex" shape enriched in LREE compare to MREE and HREE; $[La/Sm]_N$: 0.43 - 1.34; $[Sm/Yb]_N$: 0.33 - 0.55 et $[La/Yb]_N$: 0.46 - 1.28). Multi-element REE patterns of harzburgite NK04 point out a deep negative anomalies of Sr and Rb and positive anomalies in Nb and Ba.

6. Discussion: Evidence of Lake Nyos Mantle Percolated by Alkaline Magmas and Characterization of Induced Enrichment Phenomena

6.1. Magmatic Trace Infiltrations in Nyos Upper Mantle

Major element compositions of minerals are consistent with normal equilibration of typical minerals formed in the upper mantle except those of wehrlite. Indeed, olivine of wehrlite is slightly poor in Fe (Fo_{79}) compare to those (Fo_{90}) of depleted residual lherzolites [34] or olivine primitive mantle [37]. The low Fo values of olivines can be impute to the re-equilibration between olivine and a liquid rich in Fe [38] or to mantle metasomatism generated by basaltic magma infiltrations ("Fe-Ti metasomatism" [39] [40]. These low values also suggest that after their formation, wehrlite were percolated by, and re-equilibrated within basaltic magmas outled by low degrees of partial melting. Similar processes of re-equibration of wehrlite with magma of moderate Mg# have been proposed by Berger and Vannier [41] in order to explain the presence of dunites enclosed in

oceanic island alkaline basalts. The same processes were proposed by Bodinier *et al.* [42] for Lanzo dunites.

Altogether, Nyos wehrlite represents mantle residues forms by "magmatic impregnation" [38], *i.e.* solid residus were percolated by a basaltic magma, enabling Cpx to crystallize in interstices between olivine crystals. Traped magmas, out of percolator filters, contribute to the formation of wehrlite. The percolating basaltic liquids were probably formed in deep seated zone by partial melting of a lherzolitic peridotite. The percolation of peridotites by basaltic magmas may be responsible of olivine CaO abnormal enrichments in wehrlite NK08 (mean composition CaO = 0.45), conferring them a magmatic origin whereas they are primary of mantle origin. Evidence of liquid percolation and associated dissolution/recrystallisation processes are attested by the presence of glass veins in wehrlite NK08 [43], coupled with the diminution of Mg# ratio of minerals (consequently the magnesium content of the magma plummets is poor) and the LREE enrichment of Cpx (≥10% chondrites, (**Figure 6**) which is generally related to the "chromatographic effects" of melt percolation, in mixture with magmatic liquid of alkaline affinity rich in LREE [44] [45] [46]. The major element features of olivine and clinopyroxene of the wehrlite appear to be significantly different than those of their equivalents in the other peridotites. They are indeed less magnesian (Fo: 78.75 - 79.17) vs Fo (86.44 - 87.95); Mg#Cpx: (77.08 - 78.93 vs 86.93 - 90.49), the olivine is higher in CaO (0.16 - 0.33 vs 0.05 - 0.12) and the clinopyroxene displays much higher Al_2O_3 (7.63 - 8.48 vs 3.15 - 4.7) and TiO_2 (1.6 - 1.9 vs 0.17 - 0.76) contents and a lower Cr_2O_3 content (0.09 - 0.19 vs 0.61 - 1.16).

High NiO contents of harzburgites in some cases have been attributed to the re-equilibration between olivine and a liquid rich in Fe [38] [47].

The genesis of mantle amphibole is generally considered as a result of interactions between magma or a fluid and it surroundings. Interactions may be as a result of mantle metasomatism initiated by the percolation between a magma or a fluid rich in H_2O, Ti, Fe, Na, K and others incompatible elements through peridotites [15] [38] [48] [49] [50]. A similar process may justify the presence of pargasites in harzburgite NK02.

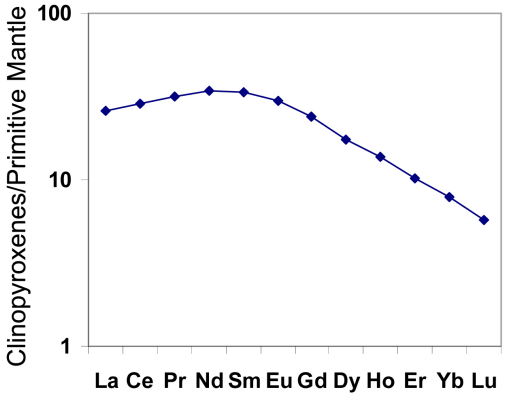

Figure 6. Clinopyroxenes REE patterns of Nyos wehrlite NK08.

The occurrence of phlogopites in fluid inclusions containing Na, K, Cl, P, and S, coupled with the fact that phlogopite and amphibole have similar trace element patterns, (their enriched in LREE and MREE compared to HREE which are nearly constant) suggest that incompatible element-enriched hydrous fluids/melts fluxed this part of the upper mantle beneath the CVL.

6.2. Metasomatic Events

The systematic investigations concerning the mineralogical and geochemical fingerprints of mantle metasomatism beneath Lake Nyos have been thorouhgfully debated (see Teitchou *et al.* [11] and associated figure captions). We therefore resume the main results in relation with the magmatic infiltration signature.

Trace element variations in mineral phases of Nyos peridotites seem more important in clinopyroxenes with two main types of REE patterns indicating different degrees of partial melting and enrichment processes by fluids (metasomatism). Indeed, Nyos clinopyroxene trace element compositions of type 1) are consistent with partial melting residues while trace element compositions of type 2) are not expressive with a simple partial melting process characterize by a systematic depletion in LREE and MREE compare to HREE [15] [35] [46] [51] [52]. Enrichments in LREE are geochemical fingerprints of metasomatism generate by the circulation and reaction with magmas (or fluids) in more or less residual mantle peridotites [15] [38] [46] [47]. This type of pattern usually appoints metasomatic enrichments later on partial melting [15] [40]. Metasomatism can be modal (by hydrous melts) and generate new hydrous mineral phases like phlogopites and pargasites [15] [38] [53] [54] or cryptic (anhydrous) characterize simply by chemical modifications (e.g, enrichments in LREE). This suggests that pargasites of sample NK02 and phlogopites of sample NK04 are witnesses of modal metasomatism. The metasomatic liquid which percolated the lithospheric column was a densely silicate rich in volatile and able to transport a high quantity of Ti, confirm by positive anomalies of Ti in harzburgites. The presence of amphibole is therefore reliable to the magmatic episode which brought out these xenoliths.

The following results were evidenced [4]:

- Clinopyroxenes are the main hosts of trace elements during partial melting of Nyos peridotites.
- The HFSE depletion trends appear to reflect low HFSE abundances in the metasomatic hydrous melts compared to the LILE, consequently, the flux of HFSE through the mantle wedge was low, corroborate by high LREE/HFSE and LILE/HFSE ratios.
- Anhydrous metasomatised peridotites experience enrichments only in HFSE melts while hydrous metasomatised peridotites experienced both enrichment in HFSE and alkali melts.
- Clinopyroxenes, amphiboles and phlogopites are good reservoirs of HFSE of the studied peridotites while REE budget is shared by amphiboles and clinopyroxenes, confirm by their parallel REE patterns enriched in LREE com-

pared to constant MREE and HREE, and also by their strong positive anomalies in Sc, Th and La and negative anomalies in Ti and Ta.

- Major element distribution in minerals reveals also the fundamental action of partial melting and metasomatic events due to percolation through peridotites of a liquid rich in H_2O, Ti, Fe, Na and K (Fe-Ti metasomatism), mineralogically recorded by pargasitic amphiboles. Partial melting and metasomatism events are also documented by bulk rock REE patterns and overall trace element in minerals, particularly clinopyroxenes which can be consider as major hosts of trace elements in Nyos peridotites. The presence of pargasite in Nyos peridotites indicates an important metasomatic event beneath the Nyos volcano. Its Ti contents, relatively high (Ti > 0.4), implies that the metasomatic agent was a silicate liquid rich in volatile than low density, H_2O-CO_2 rich fluid, unable to transport an important quantity of Ti [55]. The significant variations of K, Cr and Ti contents combine with the high Mg# ratio of pargasite are the direct consequences of the crystallization of this mineral in interstices between the mineralogical assemblage made up of olivine + clinopyroxene + spinelle. Pargasites K, Cr, Ti, Mg and Fe contents thus depend both on the composition of metasomatic liquid and previous silicate phases in the upper mantle. Therefore, the presence of amphibole, even in small amount in Nyos peridotites (modal compositions < 2%) may be reliable to alkali magmatism which brought out these peridotites. REE data indicates that peridotites without amphibole are also enriched in LREE. In addition, their $(Ce/Sm)_N$ ratio range between 1.5 - 2.5 and $(Ce/Yb)_N$ ratio range between 1 - 2 are similar to those resulting from the percolation by basaltic magmas, during or after the partial melting [56].

Harzburgites and some lherzolites display low Fe content (<0.10) but high in samples NK04 and NK14 (0.12 and 0.20 respectively). The enrichment in incompatible elements of sample NK04 is due to the presence of phlogopite which reflects modal metasomatism while sample NK14 is a "Fe-Ti" metasomatic fingerprint, recorded by primary clinopyroxenes. Those characteristics are in agreement with the fact that sample NK14 (lherzolites transitional porphyroclastic to equigranular) and the phlogopite-bearing harzburgite NK04 are metasomatised mantle peridotites whereas the wehrlite NK08 is a magmatic cumulate.

6.3. Nature of the Percoling/Metasomatizing Liquid

Petrogeochemical data on CVL Lavas indicate three mains series: 1) series of tholeitic affinity [7] [8] [57], 2) series of transitional affinity [58] [59] [60] [61] and 3) series of alkaline affinity [4] [62] [63]. The transitional series, seem older (51 - 40 Ma; [61] than the alkaline series (40 Ma to present; Nana [6]). The succession of magmas evolving in time from tholeitic, transitional to more typical alkaline compositions is still debated, allowing us to open the debate on the magmatic affinity of the metasomatizing agent that percolate the Nyos mantle column.

Data obtained from earlier work evidence the alkaline affinity of liquids reacted with peridotites of Nyos upper mantle. These findings are consistent with: 1) high contents of Al and Ti of the clinopyroxenes of wehrlite NK08; 2) crystallysation of amphibole in harzburgite NK02; 3) formation of wehrlite rich in CaO; 4) LREE enrichments (in some sample) patterns typical of upper mantle infiltrated by alkaline magmas and 5) enrichment or depletion transitional trace element in most minerals phases, particulary Ti (olivine, amphibole, phlogopite) and V (clinopyroxene) enrichments and 6) depletion in Ni both in wehrlite and lherzolite-harzburgite series. The metasomatic melts that has affected the samples NK04 and NK14 is also probably the parental melt of the wehrlite cumulate. These findings are in agreement with the fact that sample NK14 (lherzolites transitional porphyroclastic to equigranular) and the phlogopite-bearing harzburgite NK04 are metasomatised mantle peridotites whereas the wehrlite NK08 is a magmatic cumulate.

In order to test the alkaline affinity of the magma or fluid react with Nyos peridotites showing clear evidence of metasomatism (Group 2 samples): harzburgite bearing phlogopite NK04; lherzolite transitional porphyroclastic to equigranular NK14; wehrlite NK08 and precisely to test if the metasomatising magma/fluid displays similar characteristics with the alkaline lavas of the Kumba plain whose volcanism is comparable to Nyos volcanism [4]. REE contents of the theorical liquid in equilibrium with clinopyroxenes of metasomatised xenoliths were calculated. We used partition coefficients Clinopyroxene/mafic silicate liquid compilated by Chazot *et al.* [64]. Calculation were made exclusively on REE because they concentrate preferentially on clinopyroxene of anhydrous peridotites and their REE contents can be considered as reflecting the composition of the metasomatizing agent (magma/fluid). Others incompatible trace elements like LILE (Rb, Ba, Th, U, Pb) or HFSE (Nb, Ta, Ti , Zr, Hf) may preferentially concentrate in other metasomatic phases like amphibole, phlogopite or microphases (e.g. oxides) which may triggered sub-solidus equilibration processes between these metasomatic phases, erasing the primary metasomatic history previously affected these peridotites. Calculations clearly indicate similarities between REE contents of two theorical liquids in equilibrium of metasomatised clinopyroxenes of Nyos peridotites type (ii) and the one in equilibrium with clinopyroxene of the alkaline lavas of the Kumba plain (**Figure 7**) because no in situ analyses were available for Nyos lavas. Altogether, the model evidence firmly establishes a link between the alkaline affinity of the metasomatizing agent of Nyos peridotites type (ii) and the composition of magma/liquid nearly the magmas at the origin of the volcanism of the studied area.

The degrees of partial melting previously affected type (i) peridotites were estimated at ~1% - ~5% [11]. We suggest that Nyos peridotite types (i) have experienced two types of events: 1) partial melting processes and 2) mantle metasomatism related to the percolating of depleted mantle by an alkaline silicate liquid probably rich in CO_2, regardless of his high anomalies in HFSE (Nb and Ti). High LREE/HFSE ratio in basalts and peridotites suggest that melt percolation in

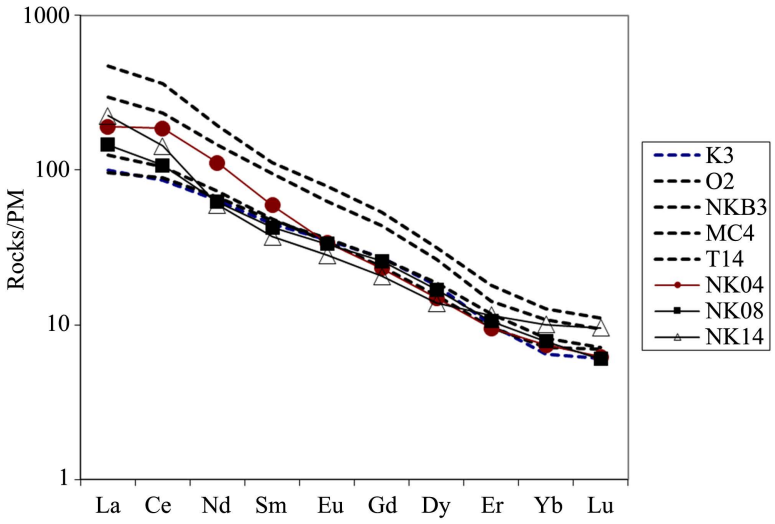

Figure 7. REE diagrams normalised [32] to primitive mantle (PM) values of theorical liquids in equilibrium with Nyos peridotites type (ii) [harzburgite bearing phlogopite NK04; lherzolite transitional porphyroclastic to equigranular NK14; wehrlite NK08], compared to those in equilibrium with clinopyroxene megacrysts of the Kumba lavas (samples K3, O2, NKB3, MC4 and T14 [4]).

xenoliths have chemical characteristic of Enriched Mantle (EM1) which is not corresponding to tectonic environments prone to tholeitic and transitional basalts characterize respectively by moderate rate of partial melting, little or no olivine in basalts and rich magnesium content of the magma plummets (not recorded in our samples).

The depth of reactive melt migration in which melt is penetrating into the protolith and reacting with it is still to be studied. Nevertheless, from the chemical evolution described above coupled with the fact that sample NK14 displays pyroxene-Cr spinel symplectites interpreted as old garnet [65]. It is suggested that in the deeper parts of the Nyos upper mantle, garnet may be a possible potassium-bearing mineral. At shallower levels of the Nyos upper mantle, (e.g. less than 40 km) amphibole may be a potassium-bearing mineral instead of or in addition to phlogopite, while in the transitional context should be probably the formation of olivine poor-host basalts (not yet described in Nyos area) fluxed by EM1 components and the absence of wehrlites respectively at deeper and shallower levels of the mantle beneath the Nyos volcano.

7. Conclusion

To sum up, sample NK 14 corresponding to lherzolite transitional porphyroclastic to equigranular, wehrlite NK08 and hydrous harzburgites (harzburgites bearing phlogopites or pargasites) display particular mineralogical characters compared to lherzolites and anhydrous harzburgites and therefore documented uplifting of the mantle and interactions between initial peridotitic upper mantle (lherzolites and harzburgites) and infiltrated basaltic magmas of alkaline affinity. These interaction processes triggered the formation of wehrlite. Thus, wehrlite NK08 corres-

ponds to products of interactions between percolating basaltic magmas and encasing mantle peridotites and then represents percolated peridotitic vents in which Opx, a member of the primary lherzolitic or harzburgitic mineral association, were quasi consumed during interactions with percolated magmas [66]. The study of these peridotites reveals a complex evolution of Nyos upper mantle which involved at least two stages. The first one was due to partial melting which produce depleted lherzolites and more refractory harzburgites from a fertile lherzolitic mantle. Later on, hydrous phases, Ti-rich Cpx, CaO rich Ol, Ti and V rich Ol wehrlite precipited from alkali enrichments due to the percolation of the mantle by basaltic magmas. Metasomatism of the upper mantle beneath Nyos probably occurred prior to recent alkaline magmatism and after the initial volcanism which formed the wehrlite cumulates. Metasomatism caused overall oxidation of the upper mantle beneath this area but probably was not responsible for the anomalously Fe-rich nature of some xenoliths attributable to the infiltration of alkaline magmatic fluid/melts beneath the lake eruptive centre.

Acknowledgements

This work was supported by a French government visiting researcher grant and the Institute of Geological and Mining Research, IRGM Cameroon. C. Dantas, Kamani Toko, and Dr. Diouta G of ISTIC Bangangte are thanked for their collaboration.

Conflicts of Interest

The authors declare no conflicts of interest regarding the publication of this paper.

References

[1] Moreau, C., Regnoult, T.M., Déruelle, B. and Robineau, B. (1987) A New Tectonic Model for Cameroon Line, Central Africa. *Tectonophysics*, **139**, 317-334. https://doi.org/10.1016/0040-1951(87)90206-X

[2] Déruelle, B., Moreau, C., Nkoumbou, C., Kambou, R., Lissom, J., Njonfang, E., Ghogomu, R.T. and Nono, A. (1991) The Cameroon Line: A Review. In: Kampunzu, A.B. and Lubala, R.T., Eds., *Magmatism in Extensional Structure Setting*, Springer-Verlag, Heidelberg, 274-328. https://doi.org/10.1007/978-3-642-73966-8_12

[3] Meyers, J.B., Rosendahl, B.R., Harrison, C.G.A. and Zan-Dong, D. (1998) Deep-Imaging Seismic and Gravity Results from the Offshore Cameroon Volcanic Line, and Speculation of African Hotlines. *Tectonophysics*, **284**, 31-63. https://doi.org/10.1016/S0040-1951(97)00173-X

[4] Teitchou, M.I. (2008) Volcanologie, pétrologie et géochimie comparées de quelques plaines continentales (Kumba, Tombel, Noun, Nyos) de la Ligne du Cameroun. Ph.D Thesis, University of Yaoundé I, Yaoundé, 206 p.

[5] Temdjim, R., Boivin, P., Chazot, G., Robin, C. and Rouleau, E. (2004) L'hétérogénéité du manteau supérieur à l'aplomb du volcan de Nyos (Cameroun) révélée par les enclaves ultrabasiques. *Comptes Rendus Geoscience*, **336**, 1239-1244.

https://doi.org/10.1016/j.crte.2004.07.005

[6] Nana, R. (2001) Pétrologie des péridotites en enclaves dans les basaltes alcalins récents de Nyos: Apport à la connaissance du manteau supérieur de la Ligne du Cameroun. Thèse doctorat d'Etat Université Yaoundé I, Yaoundé, 250 p.

[7] Aka, F.T., Nagao, K., Kusakabe, M. and Ntepe, N. (2009) Cosmogenic Helium and Neon in Ultramafic Xenoliths from the Cameroon Volcanic Line (West Africa): Preliminary Observations. *Journal of African Earth Sciences*, **55**, 175-184. https://doi.org/10.1016/j.jafrearsci.2009.04.002

[8] Aka, FT, Hasegawa, T., Nche, L.A., Asobo, N.E.A., Mimba, M.E., Teitchou, I., Ngwa, C.N., Miyabuchi, Y., Kobayashi, T., Kankeu, B., Yokoyama, T., Tanyileke, G., Ohba, T., Hell, J.V. and Kusakabe, M. (2018) Upper Triassic Mafic Dykes of Lake Nyos, Cameroon (West Africa) I: K-Ar Age Evidence within the Context of Cameroon Line Magmatism, and the Tectonic Significance. *Journal of African Earth Sciences*, **141**, 49-59. https://doi.org/10.1016/j.jafrearsci.2018.02.001

[9] Marzoli, A., Picirillio, E.M., Renne, P.R., Bellieni, G., Iacumin, M., Nyobe, J.B. and Tongwa, A.F. (2000) The Cameroon Volcanic Line Revisited: Petrogenesis of Continental Basaltic Magmas from Lithospheric and Asthenospheric Mantle Sources. *Journal of Petrology*, **41**, 87-109. https://doi.org/10.1093/petrology/41.1.87

[10] Teitchou, M.I., Grégoire, M., Dantas, C. and Tchoua, F.M. (2007) Le manteau supérieur à l'aplomb de la plaine de Kumba (ligne du Cameroun), d'après les enclaves de péridotites à spinelles dans les laves basaltiques. *Comptes Rendus Geoscience*, **339**, 101-109. https://doi.org/10.1016/j.crte.2006.12.006

[11] Teitchou, M.I., Grégoire, M., Temdjim, R., Ghogomu, R.T., Ngwa, C. and Aka, F.T. (2011) Mineralogical and Geochemical Fingerprints of Mantle Metasomatism beneath Nyos Volcano (Cameroon Volcanic Line). In: Beccaluva, L., Bianchini, G. and Wilson, M., Eds., *Volcanism and Evolution of the African Lithosphere*, Geological Society of America Boulder, Special Paper 478, 193-210. https://doi.org/10.1130/2011.2478(10)

[12] Streckeisen, A. (1976) To Each Plutonic Rock Its Proper Name. *Earth-Science Reviews*, **12**, 1-33. https://doi.org/10.1016/0012-8252(76)90052-0

[13] Boivin, P. (1982) Interactions Entre Magmas Basaltiques et Manteau Supérieur. Arguments apportés par les enclaves basiques des basaltes alcalins. Exemples de Devès (Massif Central Français) et du volcanisme quaternaire Carthagène (Espagne). Thèse d'état, Université de Clermont II, 344 p.

[14] Neumann, E.R. and Wulff-Pederson, E. (1997) The Origin of Highly Silicic Melts in the Mantle Xenoliths from the Canary Islands. *Journal of Petrology*, **38**, 1513-1539. https://doi.org/10.1093/petroj/38.11.1513

[15] Grégoire, M., Moine, B.N., O'Reilly, S.Y.., Cottin, J.Y. and Giret, A. (2000) Trace Element Residence and Partitioning in Mantle Xenoliths Metasomatized by Highly Alcaline, Silicate and Carbonate Rich Melts (Kerguelen Islands, Indian Ocean). *Journal of Petrology*, **41**, 477-509. https://doi.org/10.1093/petrology/41.4.477

[16] Remaïdi, M. (1993) Etude pétrologique et géochimique d'une association de péridotites réfractaires-pyroxénites dans le massif de Ronda (Espagne). Implications pour les mécanismes de circulation des magmas dans le manteau supérieur. Thèse Université de Montpellier, Montpellier, 360 p.

[17] Pouchou, J.L. and Pichoir, F. (1984) A New Model for Quantitative X-Ray Micro-Analysis: Part I. Application to the Analysis of Homogeneous Samples. *Recherche Aérospatiale*, **5**, 13-38.

[18] Dantas, C., Ceuleneer, G., Grégoire, M., Python, M., Freydier, R., Warren, J. and

Dick, H.B.J. (2007) Pyroxenites Dredged along the South-West Indian Ridge, 9°-16°E: Cumulates from Incremental Melt Fractions Produced at the Top of a Cold Melting Regime. *Journal of Petrology*, **48**, 647-660. https://doi.org/10.1093/petrology/egl076

[19] Bonati, E. and Michael, J. (1989) Mantle Peridotite from Continental Rifts to Ocean Basin to Subduction Zones. *Earth and Planet Science Letters*, **91**, 297-311. https://doi.org/10.1016/0012-821X(89)90005-8

[20] Tamura, A. and Arai, S. (2006) Harzburgite-Dunite-Orthopyroxenite Suite as Record of Supra-Subduction Zone Setting for the Oman Ophiolite Mantle. *Lithos*, **90**, 43-56. https://doi.org/10.1016/j.lithos.2005.12.012

[21] Nixon, P.H. (1987) Mantle Xenoliths. John Wiley and Sons, Chichester, 844 p.

[22] Caldeira, R. and Munhá, J.M. (2002) Petrology of Ultramafic Nodules from São Tomé Island, Cameroon Volcanic Line (Oceanic Sector). *Journal of African Earth Sciences*, **34**, 231-246. https://doi.org/10.1016/S0899-5362(02)00022-2

[23] Tamen, J. (1998) Contribution à l'étude géologique du plateau Kapsiki (Extrême-Nord, Cameroun): Volcanologie, pétrologie et géochimie. Thèse 3ème cycle Univrsité Yaoundé I, Yaoundé, 127 p.

[24] Princivalle, F., Salviulo, G., Marzoli, A. and Picccirillo, E.M. (2000) Clinopyroxene of Spinel-Peridotite Xenoliths from Lake Nji (Cameroon Volcanic Line, W Africa): Crystal Chemistry and Petrological Implications. *Contributions to Mineralogy Petrology*, **139**, 503-508. https://doi.org/10.1007/s004100000151

[25] Menzies, M.A. and Hawkesworth, C.J. (1987) Mantle Metasomatism. Academic Press, London, 472 p.

[26] Clague, D.A. (1988) Petrology of Ultramafic Xenoliths from Loihi Seamount, Hawaï. *Journal of Petrology*, **29**, 1161-1186. https://doi.org/10.1093/petrology/29.6.1161

[27] Girod, M., Dautria, J.-M., Ball E. and Soba D. (1984) Estimation de la profondeur du Moho, sous le massif volcanique de l'Adamaoua (Cameroun), à partir de l'étude d'enclaves de lherzolite. *Comptes Rendus Geoscience*, **298**, 699-704.

[28] Leake, B.E. (1978) Nomenclatures of Amphiboles. The *American Mineralogist*, **63**, 1023-1052.

[29] Zerka, M. (2004) Le manteau sous la marge Maghrébine: Relations infiltrations-réactions-cristallisations et cisaillements lithosphériques dans les enclaves ultramafiques du volcanisme alcalin plio-quaternaire d'Oranie, exemple des complexes d'Aïn-Temouchent et de la Basse Tafna (Algérie nord-occidentale). Thèse Doctorat d'Etat, Université Oran, Oran, 345 p.

[30] Fabriès, J., Bodinier, J.L., Dupuy, C., Lorand, J.P. and Benkerrou, C. (1989) Evidence for Modal Metasomatism in the Orogenic Spinel Lherzolite Body from Caussou (Northeastern Pyrénées, France). *Journal of Petrology*, **30**, 199-228. https://doi.org/10.1093/petrology/30.1.199

[31] Zerka, M, Cottin, J.Y., Grégoire, M., Lorand, J.P., Mergartsi, M. and Midoum, M. (2002) Les xénolites ultramafiques du volcanisme alcalin quaternaire d'Oranie (Tell, Algérie Occidentale), témoins d'une lithosphère cisaillée et amincie. *Comptes Rendus Geoscience*, **334**, 387-394. https://doi.org/10.1016/S1631-0713(02)01771-6

[32] McDonough, W.F. and Sun, S.-S. (1995) The Composition of the Earth. *Chemical Geology*, **120**, 223-253. https://doi.org/10.1016/0009-2541(94)00140-4

[33] Weber, B. (1991) Interactions basalte-lithosphère mantellique en contexte intraplaque océanique: Exemple du tahiti et Tahaa (plaque rigide) et de la Réunion (plaque

lente). Thèse d'Université, Ecole des Mines de Paris, Paris, 222 p.

[34] Jagoutz, E., Palme, H., Baddenhauser, H., Blum, K.,Cendales, M., Dreibus, G., Spettel, B., Lorenz, V. and Wänke, H. (1979) The Abundance of Major, Minor and Trace Elements in the Earth's as Derived from Primitive Ultramafic Nodules. *Proceedings* 10*th Lunar and Planetary Science Conference*, Texas, 2031-2050.

[35] McDonough, W.F. and Frey, F.A. (1989) Rare Earth Elements in Upper Mantle Rocks. In: *Geochemistry and Mineralogy of Rare Earth Elements*, *Review in Mineralogy*, *Vol.* 21, Mineralogical Society of America Publ., London, 99-139. https://doi.org/10.1515/9781501509032-008

[36] Siena, F., Beccaluva, L., Colcorti, M., Marchesi, S. and Morra, V. (1991) Ridge to Hot Spot Evolution of the Atlantic Lithosphere Mantle: Evidence from Lanzarote Peridotite Xenoliths (Canary Islands). *Journal of Petrology*, 271-290. https://doi.org/10.1093/petrology/Special_Volume.2.271

[37] Sun, S.S. and McDonough, W.F. (1989) Chemical and Isotopic Systematics of Oceanic Basalts: Implications for the Mantle Composition and Processes. In: Saunders, A.D. and Norry M.J., Eds., *Magmatism in the Oceanic Basin*, Geological Society, London, Special Publications, Blackwell Scientific Publications, Oxford, 313-346. https://doi.org/10.1144/GSL.SP.1989.042.01.19

[38] Girardeau, J. and Francheteau, J. (1993) Plagioclase-Wehrlites and Peridotites on the East Pacific Ridge (Hess Dufi) and the Mid Atlantic Ridge (DSPP Sole, 33W): Evidence for Magma Percolation in the Oceanic Upper Mantle. *Earth and Planetary Science Letters*, **115**, 137-149. https://doi.org/10.1016/0012-821X(93)90218-X

[39] Menzies, M.A., Arculus, R.J., Best, M.G., Bergman, S.C., Ehrenberg, S.N., Irving, A.J., Roden, M.F. and Schule, D.J. (1987) A Record of Subduction Processes and Within-Plate Volcanism of the Southern USA. In: Nixon, P.H., Ed., *Mantle Xenoliths*, John Wiley Sons, Chichester, 41-58.

[40] Bodinier, J.-L., Vasseur, G., Vernières, J., Dupuy, C. and Fabriès, J. (1990) Mechanism of Mantle Metasomatism: Geochemical Evidence from the Lherz Orogenic Peridotite. *Journal of Petrology*, **31**, 597-628. https://doi.org/10.1093/petrology/31.3.597

[41] Berger, E.T. and Vannier, M. (1984) Les dunites en enclaves dans les basaltes des îles océaniques: Approche pétrologique. *Bulletin of Mineralogy*, **107**, 649-663. https://doi.org/10.3406/bulmi.1984.7809

[42] Bodinier, J.-L. (1988) Geochemistry and Petrogenesis of the Lanzo Peridotite Body, Western Alps. *Tectonophysics*, **149**, 67-88. https://doi.org/10.1016/0040-1951(88)90119-9

[43] Touret, J., Gregoire, M. and Teitchou, M.I. (2010) Was the Letal Eruptrion of Lake Nyos Relted to Double CO_2/H_2O Density Inversion? *Comptes Rendus Geosciences*, **341**, 19-26. https://doi.org/10.1016/j.crte.2009.10.005

[44] Navon, O. and Stopler, E. (1987) Geochemical Consequences of Melt Percolation: the Upper Mantle as a Chromatographic Column. *Journal of Geology*, **95**, 285-307. https://doi.org/10.1086/629131

[45] Ionov, D.A., Bodinier, J.-L., Mukasa, S.B. and Zanetti, A. (2002) Mechanism and Sources of Mantle Metasomatism: Major and Trace Element Compositions of Peridotites Xenoliths from Spitsbergen in the Context of Numerical Modelling. *Journal of Petrology*, **43**, 2219-2259. https://doi.org/10.1093/petrology/43.12.2219

[46] Ionov, D.A., Chazot, G., Chauvel, C., Merlet, C. and Bodinier, J.L. (2006) Trace Elements in Peridotite Xenoliths from Tok, SE Siberian Craton: A Record of Pervasive, Multi-Stage Metasomatism in Shallow Refractory Mantle. *Geochimica et Cos-*

mochimica Acta, **70**, 1231-1260. https://doi.org/10.1016/j.gca.2005.11.010

[47] Girardeau, J. and Mercier, J-C. (1988) Petrology and Texture of the Ultramafic Rocks of the Ngaze Ophiolite (Tibet). Constraints for Mantle Structure beneath Slow-Spreading Ridges. *Tectonophysic*s, **47**, 35-58. https://doi.org/10.1016/0040-1951(88)90146-1

[48] Menzies, M.A. (1983) Mantle Ultramafic Xenoliths in Alkaline Magma: Evidence for Heterogeneity Modified by Magmatic Activity. In: Hawkesworth, C.J. and Norry, M.J., Eds., *Continental Basalts and Mantle Xenolith*, Shiva Publ., Nantwich, 92-110.

[49] Moine, B.N., Grégoire, M., O'Reilly, S., Sheppard, S.M.F. and Cottin, J.Y. (2001). High Field Strength Element (HFSE) Fractionation in the Upper Mantle: Evidence from Amphibole-Rich Composite Mantle from the Kerguelen Islands (Indian Ocean). *Journal of Petrology*, **42**, 2145-2167. https://doi.org/10.1093/petrology/42.11.2145

[50] Colcorti, M., Beccaluva, L., Bonadiman, C., Salvini, L. and Siena, F. (2000) Glasses in Mantle Xenolith as Geochemical Indicators of Metasomatic Agents. *Earth and Planetary Science Letters*, **183**, 303-320. https://doi.org/10.1016/S0012-821X(00)00274-0

[51] Grégoire, M., Lorand, J.P., Cottin, J.Y., Giret, A., Mattielli, N. and Weiss, D. (1997) Xenoliths Evidence for a Refractory Oceanic Mantle Percolated by Basaltic Melts beneath the Kerguelen Archipelago**.** *European Journal of Mineralogy*, **9**, 1085-1100. https://doi.org/10.1127/ejm/9/5/1085

[52] Bjerg, E.A., Ntaflos, T., Kurat, G., Dobosi, G. and Labudia, C.H. (2005) The Upper Mantle beneath Patagonia, Argentina, Documented by Xenoliths from Alkali Basalts. *Journal of South American Earth sciences*, **18**, 125-145. https://doi.org/10.1016/j.jsames.2004.09.002

[53] Neumann, E.R. (1991) Ultramafic and Mafic Xenoliths from Hiero, Canary Islands: Evidence for Melt Percolation in the Upper Mantle. *Contributions to Mineralogy and Petrology*, **106**, 236-252. https://doi.org/10.1007/BF00306436

[54] Kalfoum, F., Ionov, D. and Merlet, C. (2002) HFSE Residence and Nb-Ta Ratios in Metasomatised, Rutile Bearing Mantle Peridotites. *Earth and Planetary Science Letters*, **199**, 49-65. https://doi.org/10.1016/S0012-821X(02)00555-1

[55] Eggler, D.H. (1987) Enrichment Processes and Basaltic Volcanism. In: Menzies, M.A. and Hawkesworth, C.J., Eds., *Mantle Metasomatism*, Academic Press, London, 21-39.

[56] Luguet, A., Alard, O., Lorand, J.P., Perason, N.J., Ryau, C. and O'Reilly, S. (2001) Laser-Ablation Microprobe (LAM-ICPMS) Unravels the Highly Siderophile Element Geochemistry of Oceanic Upper Mantle. *Earth and Planetary Science Letters*, **189**, 285-294. https://doi.org/10.1016/S0012-821X(01)00357-0

[57] Klamadji, M.N., Dedzo, M.G., Tchameni, R. and Dawaï, D. (2020) Petrography and Geochemical Characterization of Dolerites from Figuil (Northern Cameroon) and Léré (Southwestern Chad). *International Journal of Geosciences*, **11**, 459-482. https://doi.org/10.4236/ijg.2020.117023

[58] Moundi, A., Ménard, J.-J., Reusser, E., Tchoua, F.M. and Dietrich, V.J. (1996) Découverte de basaltes transitionnels dans le secteur continental de la Ligne du Cameroun (Massif du Mbam, Ouest-Cameroun). *Comptes Redus Academie. Sciences. Paris*, **322**, 831-837.

[59] Fosso, J., Ménard, J.-J., Bardintzeff, J.-M., Wandji, P., Tchoua, F.M. and Bellon, H. (2005) Les laves du mont Bangou: Une première manifestation volcanique éocène, à

affinité transitionnelle, de la Ligne du Cameroun. *Comptes Rendus Geosciences*, **337**, 315-325. https://doi.org/10.1016/j.crte.2004.10.014

[60] Kuepouo, G., Tchouankoue, J.P., Nagao, T. and Sato, H. (2006). Transitional Tholeiitic Basalts in the Tertiary Bana Volcano-Plutonic Complex, Cameroon Line. *Journal of African Earth Sciences*, **45**, 318-332. https://doi.org/10.1016/j.jafrearsci.2006.03.005

[61] Moundi, A., Wandji, P., Bardintzeff, J.-M., Ménard, J.-J., Okomo Atouba, L.C., Mouncherou, O.F. and Tchoua, F.M. (2007) Les basaltes éocènes à affinité transitionnelle du plateau Bamoun, témoins d'un réservoir mantellique enrichi sous la ligne volcanique du Cameroun. *Comptes Rendus Geoscience*, **339**, 396-406. https://doi.org/10.1016/j.crte.2007.04.001

[62] Kagou Dongmo, A., Wandji, P., Poucle, A., Vicat, J.-P., Cheilletz, A., Nkouathio, D.G., Alexandrov, P. and Tchoua, F.M. (2001) Evolution volcanologique du mont Manengouba (Ligne du Cameroun): Nouvelles données pétrographiques, géochimiques et géochronologiques. *Comptes Rendus Géosciences*, **333**, 155-162. https://doi.org/10.1016/S1251-8050(01)01625-1

[63] Ngongang, N., Wagsong, M., Owono, F., Badriyo, I., Essomba, P., Tchikankou, N., Youmen, D., Kamgang, P. and Chazot, G. (2021) Mineralogy and Magmatic Processes of Cenozoic Intraplate Alkaline Volcanic Rocks of Bafang and Its Environs (Cameroon Volcanic Line, West Africa). *Open Journal of Geology*, **11**, 210-238. https://doi.org/10.4236/ojg.2021.116013

[64] Chazot, G., Menzies, M.A. and Harte, B. (1996) Determination of Partition Coefficients between Apatite, Clinopyroxene, Amphibole and Melt in Natural Spinel Lherzolites from Yemen: Implication for Wet Melting of the Lithospheric Mantle. *Geochimica et Cosmochimica Acta*, **60**, 423-437. https://doi.org/10.1016/0016-7037(95)00412-2

[65] Darwson, J.B. (1984) Constrasting Types of Upper Mantle Metsomatism. In: Kornprobst, J., Ed., *Kimberlites II. The Mntle Crust Relationship*, Elsevier, Amsterdam, 289-294. https://doi.org/10.1016/B978-0-444-42274-3.50030-5

[66] Patkó, L., Liptai, N., Aradi, L.E., Klébesz, R., Sendula, E., Bodnar, R.J. and Szabó, C. (2019) Metasomatism-Induced Wehrlite Formation in the Upper Mantle beneath the Nógrád-Gömör Volcanic Field (Northern Pannonian Basin): Evidence from Xenoliths. *Geoscience Frontiers*, **11**, 943-964. https://doi.org/10.1016/j.gsf.2019.09.012